ZU-TH 04/03

Probing neutrino mass with multilepton production at the Tevatron in the simplest R-parity violation model

M. B. Magro,[1,*] F. de Campos,[2,†] O. J. P. Éboli,[1,‡]
W. Porod,[3,§] D. Restrepo,[4,¶] and J. W. F. Valle[5,**]

[1]*Instituto de Física, Universidade de São Paulo, São Paulo – SP, Brazil.*

[2]*Departamento de Física e Química, Universidade Estadual Paulista - Brazil*

[3] *Institut für Theoretische Physik, Universität Zürich, Zürich, Switzerland*

[4]*Instituto de Física, Universidad de Antioquia - Colombia*

[5]*Instituto de Física Corpuscular – C.S.I.C./Universitat de València*
Edificio Institutos de Paterna, Apt 22085, E–46071 València, Spain

We analyse the production of multileptons in the simplest supergravity model with bilinear violation of R parity at the Fermilab Tevatron. Despite the small R-parity violating couplings needed to generate the neutrino masses indicated by current atmospheric neutrino data, the lightest supersymmetric particle is unstable and can decay inside the detector. This leads to a phenomenology quite distinct from that of the R-parity conserving scenario. We quantify by how much the supersymmetric multilepton signals differ from the R-parity conserving expectations, displaying our results in the $m_0 \otimes m_{1/2}$ plane. We show that the presence of bilinear R-parity violating interactions enhances the supersymmetric multilepton signals over most of the parameter space, specially at moderate and large m_0.

*Electronic address: magro@fma.if.usp.br
†Electronic address: fernando@ift.unesp.br
‡Electronic address: eboli@fma.if.usp.br
§Electronic address: porod@physik.unizh.ch
¶Electronic address: restrepo@uv.es
**Electronic address: valle@ific.uv.es

I. INTRODUCTION

Supersymmetry (SUSY) provides a promising candidate for physics beyond the Standard Model (SM). The search for supersymmetric partners of the SM particles constitutes an important item in the agenda of current high energy colliders like the Tevatron, and future colliders like the CERN Large Hadron Collider or a linear e^+e^- collider. So far most of the effort in searching for supersymmetric signatures has been confined to the framework of R-parity conserving realizations [1]; see, however, Ref. [2] and references therein.

Recent data on solar and atmospheric neutrinos give a robust evidence for neutrino conversions [3], probably the most profound discovery in particle physics in the recent years. It has been suggested long ago that neutrino masses and supersymmetry may be deeply tied together [4]. Indeed, SUSY models exhibiting R-parity violation can lead to neutrino masses and mixings [5] in agreement with the current solar and atmospheric neutrino data. Furthermore, the simplest possibility is bilinear R-parity violation [6, 7] which may arise as an effective description of a spontaneous R-parity violation scenario [8], or from some suitable `ab initio` symmetries [9].

It is interesting to notice that neutrino mass models based on R-parity violation can be tested at colliders [10, 11, 12]. In this work, we study the production of multileptons ($\geq 3\ell$ with $\ell = e$ or μ) at the Fermilab Tevatron within the framework of the simplest supergravity (SUGRA) model without R-parity conservation [7]. We show that the presence of bilinear R-parity violating (BRpV) interactions enhances the supersymmetric multilepton signals over most of the parameter space, specially at moderate and large m_0. In order to make the comparison with the R-parity conserving case easier, we performed our detailed study of the signal and SM backgrounds, adopting the same cuts (soft cuts SC2) proposed in Ref. [13].

In SUGRA with universal soft breaking terms at unification, the masses of the sleptons, the lighter chargino ($\tilde{\chi}_1^\pm$), and the lighter neutralinos ($\tilde{\chi}_1^0$ and $\tilde{\chi}_2^0$) are considerably smaller than the gluino and squark ones over a large range of the parameter space [13]. Therefore, the production of charginos and neutralinos provides the largest reach at the Tevatron. In R-parity conserving scenarios, a promising signal for SUGRA at the Tevatron is the production of $\tilde{\chi}_2^0\tilde{\chi}_1^\pm$ pairs and their subsequent decay into three charged leptons in association with missing energy due to the undetected lightest supersymmetric particle (LSP), which turns out to be $\tilde{\chi}_1^0$. In the presence of R-parity violation, the LSP is no longer stable, giving rise to events containing more particles, and it can be electrically charged since it decays. Interesting signals for such scenarios have been worked out for staus [12], stops [14], gluinos [15] and also for supersymmtric Higgs bosons [16]. The larger activity in the detector can either enhance the signal, via the production of additional leptons or suppress it due to the hadronic activity that spoils the isolation of the leptons. Therefore, a careful reanalysis of the trilepton signal is necessary.

In this work, we consider a SUGRA model that includes the following bilinear terms in the superpotential [6, 7, 17]

$$W_{\mathrm{BRpV}} = W_{\mathrm{MSSM}} - \varepsilon_{ab}\epsilon_i \widehat{L}_i^a \widehat{H}_u^b \ , \tag{1}$$

where the last term violates R parity. In order to reproduce the values of neutrino masses indicated by current neutrino data [18] we must have $|\epsilon_i| \ll |\mu|$, where μ denotes the SUSY bilinear mass parameter [5]. The relevant bilinear terms in the soft supersymmetry breaking sector are

$$V_{\mathrm{soft}} = m_{H_u}^2 H_u^{a*} H_u^a + m_{H_d}^2 H_d^{a*} H_d^a + M_{L_i}^2 \widetilde{L}_i^{a*} \widetilde{L}_i^a - \varepsilon_{ab} \left(B\mu H_d^a H_u^b + B_i \epsilon_i \widetilde{L}_i^a H_u^b \right) \ , \tag{2}$$

where the terms proportional to B_i are the ones that violate R parity. The explicit R-parity violating terms induce vacuum expectation values (vev) v_i, $i = 1, 2, 3$ for the sneutrinos, in addition to the two Higgs vev's v_u and v_d.

Our goal is to determine the impact of R-parity violation on SUSY multilepton signals, for example in the production of three or more electrons or muons, taking into account the magnitude of the mass scale indicated by the current atmospheric neutrino experiments. In phenomenological studies where the details of the neutrino sector are not relevant, it has been proven very useful to work in the approximation where R parity and lepton number are violated in only one generation [16, 19]. Thus, the first step to achieve our goal is to assume the approximation where R parity is violated only in the third generation (of course all gauge interactions are treated in the full three-generation scheme). This is the theoretically natural choice to make, since the third generation forms the basis for the radiative breaking of the electroweak symmetry, driven by the top quark Yukawa coupling. From the point of view of the analysis presented below, the breaking of R parity only in the third generation also corresponds to the worst-case-scenario: the breaking of R parity in the muon channel would produce muons directly, not just as tau decay products, leading to an enhanced multilepton (multi-muon) signal.

II. MAIN FEATURES OF OUR BRPV MODEL

The parameter space of our SUGRA model, which exhibits R-parity violation only in the third generation, is

$$m_0 \, , \, m_{1/2} \, , \, \tan\beta \, , \, \text{sign}(\mu) \, , \, A_0 \, , \, \epsilon_\tau \, , \text{and } m_{\nu_3} \, , \tag{3}$$

where $m_{1/2}$ and m_0 characterise the common gaugino mass and scalar soft SUSY breaking masses at the unification scale, A_0 is the common trilinear term, and $\tan\beta$ is the ratio between the Higgs field vev's. Although many parameterisations are possible, it is convenient to characterise the BRpV sector by the bilinear superpotential term ϵ_τ and the neutrino mass m_{ν_3}.

We considered the running of the masses and couplings to the electroweak scale, assumed to be the top mass, using the one–loop renormalization group equations. In the evaluation of the gaugino masses, we included the next–to–leading order (NLO) corrections coming from α_s, the two–loop top Yukawa contributions to the beta-functions, and threshold corrections enhanced by large logarithms; for details see [20]. The NLO corrections are especially important for M_2, leading to a change in the wino mass up to 20%. We then input the soft terms into PYTHIA that was used to evaluated the masses and decay rates of all particles, except the first and second neutralinos.

Present neutrino oscillation data fix the mass splittings among the three neutrinos, leaving arbitrary the overall scale of neutrino masses. The latter could be as large as an electron volt or so without conflicting with cosmology, beta decays and neutrinoless double beta decays, given current uncertainties in nuclear matrix element calculations [21]. However, in the BRpV model, neutrino masses are strongly hierarchical [5], specially the lightest neutrino mass. As a result the possibility of quasi-degenerate neutrinos is not realized in this model and, correspondingly, we will not discuss it any further. In what follows, whenever we fix the BRpV parameters, we take the tree level neutrino mass as $m_{\nu_3} = 0.05$ eV, the current atmospheric best fit value from Ref. [18, 22], and fix the value of the remaining BRpV parameter ϵ_τ at representative values 0.22 GeV and 7×10^{-4} GeV.

The presence of BRpV induces a mixing between the neutrinos and neutralinos, giving rise to R-parity violating decays of the LSP. In our model, the lightest neutralino presents leptonic decays $\tilde{\chi}^0_1 \to \nu \ell^+ \ell'^-$, semi-leptonic ones $\tilde{\chi}^0_1 \to \nu q \bar{q}$ or $\ell q \bar{q}$, and the invisible mode $\tilde{\chi}^0_1 \to \nu\nu\nu$ [11]. The expected $\tilde{\chi}^0_1$ lifetime and decay lengths depend both on the magnitude of R-parity breaking parameters and the chosen values of the SUGRA parameters.

Fig. 1(a) shows the lightest neutralino decay length as a function of its mass for $A_0 = 0$, $\mu > 0$, $\tan\beta = 3$, and $\epsilon_\tau = 0.22$ GeV. In this figure, the solid lines stand for the tree-level neutrino mass $m_{\nu_3} = 0.05$ eV, corresponding to the best fit atmospheric scale as given in Ref. [18], and we chose $m_0 = 200$ and 700 GeV. The bands in these figures were obtained by taking m_{ν_3} within the 3σ allowed atmospheric mass splitting of Ref. [18]. Fig. 1(b) presents the LSP decay length as a function of the neutrino mass, for different lightest neutralino masses and the parameters used in Fig. 1(a).

From Figs. 1 we can see clearly that the LSP decay length is shorter for larger neutrino and LSP masses, as expected. Furthermore, irrespective of the smallness of the neutrino mass indicated by the atmospheric oscillation data, the LSP ($\tilde{\chi}^0_1$) decays inside the detector in a large portion of the parameter space, specially for small m_0. It is interesting to notice that the kinks in Fig. 1 are associated to the opening of the LSP decays into on-shell gauge bosons.

Figure 2 contains the $\tilde{\chi}^0_1$ branching ratios as a function of $m_{1/2}$ for $\epsilon_\tau = 0.22$ GeV, $m_{\nu_3} = 0.05$ eV, $A_0 = 0$, and $\mu > 0$. As we can see from this figure, the decay $\tilde{\chi}^0_1 \to \nu b \bar{b}$ dominates at small m_0 and large $\tan\beta$. This decay channel arises from an effective coupling λ'_{333}, induced by the neutrino–neutralino mixing, which is proportional both to the bottom Yukawa coupling and to the bilinear parameter ϵ_τ in our model. Therefore, this decay is enhanced at small m_0 due to the lightness of the scalars that mediate it and at large $\tan\beta$ due to enhanced Yukawa couplings. Both features are apparent in the panels of this figure. Moreover, whenever $\tilde{\chi}^0_1 \to \nu b \bar{b}$ is not the leading channel, the LSP decays mostly to $\tau u \bar{d}$, with a sizable branching fraction $\tilde{\chi}^0_1 \to \tau \nu_\ell \bar{\ell}$.

In Fig. 3, we present the dependence of the $\tilde{\chi}^0_1$ branching ratios with respect to the R-parity violating parameter ϵ_τ. The importance of the $\nu b \bar{b}$ decay mode increases for large ϵ_τ, since the effective coupling λ'_{333} is proportional to ϵ_τ. Moreover, Fig. 4 shows that the LSP branching ratio into $\nu b \bar{b}$ decreases with increasing m_{ν_3} in the parameter regions where this mode is sizeable.

One comment is in order here, concerning the naturalness of the above branching ratio predictions. This issue depends somewhat on the assumptions about the supersymmetry soft breaking terms. We are tacitly assuming them to be universal at some unification scale. This is the usual practice and is adopted here to ensure simple comparison with the SUGRA R-parity conserving results for the trilepton signal obtained in Ref. [13]. In the BRpV model universality plays another important role, namely, it ensures "calculability" of the neutrino mass m_{ν_3}, by the renormalization group evolution. One finds in this case that the smallness of m_{ν_3} required by experiment follows naturally from the approximate "alignment" of BRpV parameters discussed, for example, in Ref. [9, 19]. In such scenario one has that the short LSP decay path is indeed technically natural, despite the small neutrino mass. However one should stress that strictly universal boundary conditions are not at all essential for the consistency of the results presented here.

Summing up, we can say that in the BRpV model the $\tilde{\chi}^0_1$ decays mainly into $\tau u d$ for large m_0 or small ϵ_τ, while its decays are dominated by $\nu b\bar{b}$ at small m_0 and large ϵ_τ ($\tan\beta$). As we will see in what follows this has important implications for the trilepton signal.

III. SIGNAL, BACKGROUNDS, AND SELECTION CUTS

In R-parity conserving scenarios, trilepton production at the Tevatron proceeds via $p\bar{p} \to \tilde{\chi}^0_2\tilde{\chi}^\pm_1$ with $\tilde{\chi}^\pm_1 \to \ell\nu\tilde{\chi}^0_1$, $\tilde{\chi}^0_2 \to \ell^+\ell^-\tilde{\chi}^0_1$, and the LSP ($\tilde{\chi}^0_1$) leaving the detector undetected. The main SM backgrounds for trilepton production are displayed in Table I. In order to suppress these backgrounds, we have imposed the soft cuts SC2 defined in Ref. [13], which were tailored for scenarios containing soft signal leptons coming from τ decays [23]:

C1: We required the presence of three isolated leptons (e or μ) with a hadronic E_T smaller that 2 GeV in a cone of size $\Delta R = 0.4$ around the lepton [24];

C2: We required the most energetic lepton to satisfy $|\eta_{\ell_1}| < 1.0$ and $p_T(\ell_1) > 11$ GeV;

C3: The second (third) most energetic lepton must satisfy $|\eta_{\ell_{2/3}}| < 2.0$ and $p_T(\ell_{2(3)}) > 7$ (5) GeV;

C4: We required the missing transverse energy to be larger than 25 GeV;

C5: We vetoed events exhibiting a $\ell^+\ell^-$ pair with an invariant mass smaller than 20 GeV and larger than 81 GeV (this avoids both Z boson and QED contributions);

C6: We vetoed events with a transverse mass of a charged lepton and missing transverse energy between 60 GeV and 85 GeV in order to suppress W decays.

In our analysis, the signal and backgrounds were generated using PYTHIA [25], except for the $WZ^\star(\gamma^\star)$ which was computed using the complete matrix elements [26]. Furthermore, we also simulate experimental resolutions by smearing the energies, but not directions, of all final state particles with a Gaussian error given by $\Delta E/E = 0.7/\sqrt{E}$ (E in GeV) for hadrons and $\Delta E/E = 0.15/\sqrt{E}$ for charged leptons.

The cross section for the SM backgrounds after cuts are shown in Table I. Notice that our results differ slightly from the ones in Ref. [13] because the hadronization procedures used in PYTHIA and ISAJET are different. Moreover, we can see that the most important background is the $t\bar{t}$ production, accounting for 70% of the total background. We further tested our code by verifying that our results for the R-parity conserving signal agree with the ones in Ref. [13].

In our BRpV model there are more SUSY reactions that can contribute to the trilepton signal than in the R-parity conserving case, since the $\tilde{\chi}^0_1$ decays can give rise to charged leptons. In the parameter range interesting for neutrino physics R-parity violating decay modes are only important for the LSP decays and can safely be neglected for the other SUSY particles. We have incorporated all possible decay modes of the lightest neutralino and the second lightest neutralino taking fully into account large tan(β) effects in PYTHIA, leaving the other decay modes unchanged. Assuming that gluinos and squarks are too heavy to be produced at the Tevatron, we considered the following processes:

$$p\bar{p} \to \tilde{\ell}\tilde{\ell}^\star \quad , \quad \tilde{\nu}\tilde{\ell} \quad , \quad \tilde{\chi}^0_i\tilde{\chi}^0_j \; (i(j) = 1,2) \quad , \quad \tilde{\chi}^+_1\tilde{\chi}^-_1 \quad , \text{and} \quad \tilde{\chi}^0_i\tilde{\chi}^\pm_1 (i = 1,2) \; .$$

The $\tilde{\chi}^0_1$ decays can contain charged leptons, and therefore, we should also analyse multi-lepton ($\geq 4\ell$) production. In order to extract this signal, we applied the cuts C1, C3, C5, and C2 but accepting leptons with $|\eta(\ell)| < 3$. We also required the presence of an additional isolated lepton with $p_T > 5$ GeV and demanded the missing transverse energy to be larger than 20 GeV. The main SM backgrounds for this process are $t\bar{t}$, WZ, and ZZ productions whose cross sections after cuts are shown in Table II.

We can see from Fig. 1 that the lightest neutralino might not decay inside the detector depending on the point of the parameter space. If it decays inside the tracking system, it can give rise to spectacular events exhibiting displaced vertices without an incoming track associated to it. In our analyses, we did not look for displaced vertices since the corresponding backgrounds depend upon details of the detector. This possibly is a conservative hypothesis since this kind of events should present a small background, leading to a larger reach of the Tevatron. Nevertheless, we kept track of the position of the neutralino decay and accepted events where the neutralino decays inside the tracking system, rejecting all events where one of the neutralinos decays outside a cylinder around the beam pipe of radius 0.5 m and length 2.0 m; we named this requirement C7. Again, this is another conservative estimate of the expected BRpV signal.

We investigated the regions of the $m_0 \otimes m_{1/2}$ plane where the trilepton and multilepton signals can be established at the Tevatron for integrated luminosities of 2 fb^{-1} and 25 fb^{-1} and fixed values of A_0 (=0), $\tan\beta$, sign(μ) (> 0), ϵ_τ, and m_{ν_3} ($= 0.05$ eV). We evolved the renormalization group equations starting at the unification scale (few $\times 10^{16}$ GeV) for the soft parameters, rejecting the points where either the electroweak symmetry is not correctly broken, or which exhibit particles with mass excluded by present experimental data [27]. In our analysis, we have employed the Poisson statistics, except when the expected number of signal events is large enough to justify the use of the Gaussian distribution [28]. We exhibit our results in the $m_0 \otimes m_{1/2}$ plane, denoting by black circles the theoretically excluded points, and by white circles the experimentally excluded by sparticle and Higgs boson searches at LEP2 [27]. The black squares represent points accessible to Tevatron experiments at 5σ level with 2 fb^{-1} of integrated luminosity, while the white squares are accessible with 25 fb^{-1}. Points denoted by diamonds are accessible only at the 3σ level with 25 fb^{-1}, while the stars correspond to the region not accessible to the Tevatron.

The trilepton cross section is always dominated by the $\tilde{\chi}_1^+\tilde{\chi}_1^-$ and $\tilde{\chi}_2^0\tilde{\chi}_1^\pm$ productions, with the second process being about 20% to 50% larger than the first. For example, these reactions are responsible for approximately 99% of the cross section at large m_0. Note that the first process can contribute to the trilepton signal only in R-parity violating scenarios. Moreover, at small and moderate m_0 ($\lesssim 400$ GeV), the $\tilde{\chi}_1^0\tilde{\chi}_1^\pm$ production is responsible for approximately 5–10% of the signal cross section and the production of sleptons also gives a sizable contribution.

To study the multilepton signal we choose three representative parameter regions. The best scenario corresponds to the case where $\tan\beta$ and ϵ_τ are small. We subsequently relax this optimistic assumption by considering separately the cases where either (but not both, since in this case the signal is too small) ϵ_τ or $\tan\beta$ are large.

In Fig. 5, we present the region of the $m_0 \otimes m_{1/2}$ plane that can be probed at the Tevatron for $\tan\beta = 3$ and BRpV parameters $\epsilon_\tau = 7 \times 10^{-4}$ GeV and $m_{\nu_3} = 0.05$ eV. For these values of the parameters, the signal cross section is dominated by $\tilde{\chi}_1^+ \tilde{\chi}_2^0$ production followed by $\tilde{\chi}_1^+ \to \tilde{\chi}_1^0 l^+ \nu$, $\tilde{\chi}_2^0 \to \tilde{\chi}_1^0 qq$ and the LSP $\tilde{\chi}_1^0$ decays mainly into $\tau u \bar{d}$. As expected, the long lifetime of the neutralino reduces considerably the signal in the shaded area of Fig. 5 after we apply the cut C7. Therefore, we might be able to further probe this region by looking for displaced vertices, and consequently enhance the Tevatron reach.

It is interesting to compare our results presented in Fig. 5 with the ones in Ref. [13]. First of all, the presence of BRpV interactions reduces the Tevatron reach in the trilepton channel for small values of m_0. This happens because there are some competing effects in this region of parameters: on the one hand there are new contributions to the trilepton process due to LSP decay and on the other hand, the decay of the neutralinos produce a larger hadronic activity, worsening the lepton isolation, and reducing the missing E_T compared with the MSSM case. Besides that, the leptons from the $\tilde{\chi}_1^0$ decay can give rise to additional isolated leptons which can contribute to the trilepton signal or, alternatively, can suppress it due to the presence of more than three isolated leptons. The last effect and the larger hadronic activity reduce the trilepton signal at small m_0 in the BRpV model. In contrast, as can be seen from Fig. 5, the trilepton reach at large m_0 always tends to increase with respect to the MSSM expectation. This follows from the fact that the drastic reduction of the $\tilde{\chi}_2^0$ branching ratio into leptons at large m_0 is compensated by the additional production of charged leptons in $\tilde{\chi}_1^0$ decays. Since these extra leptons come from tau decays, it is important to adopt cuts which increase the acceptance of soft leptons. The cuts we used satisfy this requirement.

In Fig. 6(a) we present the Tevatron reach in the multilepton (four leptons or more) channel for the same parameters adopted in Fig. 5. As we can see, the multilepton reach is larger than the trilepton one, increasing the discovery potential at large values of $m_{1/2}$. For instance, the Tevatron reach at large m_0 is $\simeq 225$ GeV in our BRpV model while it is of the order of 150 GeV in the MSSM. Moreover, unlike the trilepton signal, the discovery potential at small m_0 is also increased with respect to that of the MSSM. In this region it is clear that the reduction of the trilepton signal is largely due to the presence of additional isolated leptons. As in Fig. 5, the shaded area represent the region where displaced vertices could be used to further increase the sensitivity to BRpV. In Fig. 6(b) we present the combined results for the trilepton and multilepton searches using the chi-square criteria. It is interesting to notice that the presence of R-parity violating interactions leads to a 5σ SUSY discovery even at large m_0, a region where the usual R-parity conserving SUGRA model has no discovery potential at all. Notice the importance of combining trilepton and multilepton signals to achieve this conclusion.

Let us now consider a second scenario where the $\tilde{\chi}_1^0$ decays predominantly into $\nu_3 b\bar{b}$ at low m_0. As seen in Fig. 3, the dominance of this decay channel happens for large ϵ_τ values since the LSP decay is scalar mediated. The $\nu_3 b\bar{b}$ decay mode spoils lepton isolation, without producing any additional charged leptons and may be regarded, in a sense, as a worse case scenario in comparison with the case of small ϵ_τ and m_0. In order to illustrate this case we fixed $\epsilon_\tau = 0.22$ GeV and the remaining parameters as before; $A_0 = 0$, $\tan\beta = 3$, $\mu > 0$, and $m_{\nu_3} = 0.05$ eV. From Fig. 7 we can see that the trilepton reach is indeed further reduced at small and medium m_0, as expected. The same happens for the multilepton signal; see Fig. 8. Nevertheless, combining these signals still leads to a reach that is better than the MSSM one for all m_0 and $m_{1/2}$ values.

Finally, we consider the case of small ϵ_τ and large $\tan\beta$, say $\epsilon_\tau = 7 \times 10^{-4}$ GeV and $\tan\beta = 35$. Fig. 9 displays the Tevatron reach in the trilepton channel for this case, keeping the remaining parameters as before; $A_0 = 0$, $\mu > 0$, and $m_{\nu_3} = 0.05$ eV. For these parameters, the main $\tilde{\chi}_1^0$ decay mode is $\tau u\bar{d}$. However, there is a sizable contribution of the $\nu b\bar{b}$ channel at small m_0. As expected, the SUSY reach decreases at small m_0, specially as we increase $\tan\beta$. In contrast, there is a slight gain for $m_0 \gtrsim 200$ GeV; see Fig. 9. The similarity between the results in Fig. 5 and Fig. 9 at large m_0 can be ascribed to the τud dominance of the LSP decay; see Fig. 4(b) and Fig. 4(d). In contrast the situation is more complicated at smaller m_0 as seen in Fig. 5 and Fig. 9.

For the last choice of parameters, the Tevatron discovery potential in the multilepton channel is larger in our BRpV model than in the MSSM except at small m_0, however, it is similar to the first case we analyzed; see Fig. 10(a) and Fig. 6(a). This feature survives the combination of three and multilepton signals, as can be seen from Fig. 6(b) and Fig. 10(b). In contrast, the combined analysis does make a difference in the small m_0 region. In all cases, however, the reach of the BRpV model is larger than the MSSM one.

IV. CONCLUSION

We have analyzed the production of multileptons ($\geq 3\ell$ with $\ell = e$ or μ) in the simplest supergravity model with violation of R parity at the Fermilab Tevatron. In this model, an effective bilinear term in the superpotential parameterizes the explicit breaking of R parity. Despite the small R-parity violating couplings needed to generate the neutrino masses indicated by current atmospheric neutrino data, the lightest supersymmetric particle is unstable and can decay inside the detector. This leads to a phenomenology quite distinct from that of the R-parity conserving scenario. We have quantified by how much the supersymmetric multilepton signals differ from the R-parity conserving expectations, displaying our results in the $m_0 \otimes m_{1/2}$ plane. We have shown that the presence of bilinear R-parity violating interactions enhances the supersymmetric multilepton signals over most of the parameter space, specially at moderate and large m_0. These topologies are useful not only for discovery, but also to verify whether R parity is conserved or not.

Adopting the hadronization procedures used in PYTHIA, we have first reproduced the results for the trilepton signal expected in the conventional R-parity conserving supergravity model. We have found good agreement with the results of Ref. [13] which adopts the ISAJET event generator. We have then shown how the presence of BRpV interactions leads to a small suppression of the trilepton signal at small values of m_0 irrespective of the value of BRpV parameter ϵ_τ. This is due to the $\tilde{\chi}^0_1$ decay into $\nu b\bar{b}$. However, the $\tilde{\chi}^0_1$ decays lead to a drastically extended reach at large m_0 as a result of the LSP decay into $\tau u\bar{d}$. Moreover, the presence of additional isolated leptons in the signal allows us to look for multilepton events.

We have demonstrated that combining the trilepton and multilepton searches increases the Tevatron Run II sensitivity for most of SUGRA and R-parity breaking parameters. Note, however, that for neutrino masses in the range indicated by current atmospheric data one has a gap between the $\tilde{\chi}^0_1$ masses that can be probed at LEP2 (up to 40 GeV or so) and those that can be studied at the Tevatron (above 70 GeV or so): within this range the $\tilde{\chi}^0_1$ decay length is rather large, requiring the study of other topologies, like the presence of displaced vertices in the tracking system. It is interesting to notice that we can search for SUSY signals also in the low m_0 region by looking for events exhibiting multi jets + lepton

+ missing transverse momentum [29, 30].

In the present paper we have confined ourselves to the case in which the lightest neutralino is also the lightest supersymmetric particle [31], the most likely possibility if we adopt the simplest set of supersymmetry soft breaking terms, universal at some unification scale. We also have focused on the case where we have only one generation and this is chosen to be the third. This is done first for simplicity. Second we adopt this choice as a worse-case scenario. In other words, in those parameter regions where our multi-lepton signal can be discovered in the present one-generation approximation, the inclusion of additional generations can only improve our result. In contrast, in those regions where our results are negative, the situation is totally inconclusive in the sense that a full fledged analysis including all generations might reveal that the signal can also be detected in part of those regions. Therefore our results are robust, in the sense that the inclusion of additional generations would imply new sources of leptons, specially muons. The analysis is substantially more involved, however, than the one considered here and will be taken up elsewhere.

Acknowledgments

Research supported by Fundação de Amparo à Pesquisa do Estado de São Paulo (FAPESP), by Conselho Nacional de Desenvolvimento Científico e Tecnológico (CNPq), by Programa de Apoio a Núcleos de Excelência (PRONEX), by Spanish MCyT grant BFM2002-00345 and by the European Commission RTN network HPRN-CT-2000-00148. W.P. has been supported by the 'Erwin Schrödinger fellowship' No. J2272 of the 'Fonds zur Förderung der wissenschaftlichen Forschung' of Austria and partly by the Swiss 'National-fonds'. D.R. has been partially supported by UdeA-CODI Grant No. 381-8-10-02.

[1] Proc. of the Workshop on Physics at LEP2, CERN 96-01, Vol. I, p. 463, edited by G. Altarelli, T. Sjöstrand, and F. Zwirner, [hep-ph/9602207]; J. Amundson *et al.*, Proceedings of the 1996 DPF/DPB Summer Study on High-Energy Physics, Snowmass, Colorado, 1996, edited by D.G. Cassel, L. Trindle Gennari, R.H. Siemann, p. 655; A. Bartl *et al.*, ibid., p. 693; S. Mrenna *et al.*, ibid., p. 681; M. Carena *et al.*, hep-ex/9802006, hep-ex/9712022; ECFA/DESY LC Physics Working Group, E. Accomando et al., Phys. Rep. **299**, 1 (1998).

[2] B. Allanach *et al.*, arXiv:hep-ph/9906224; A. Datta, B. Mukhopadhyaya and F. Vissani, Phys. Lett. B **492**, 324 (2000) [arXiv:hep-ph/9910296]; B. Mukhopadhyaya, S. Roy and F. Vissani, Phys. Lett. B **443**, 191 (1998) [arXiv:hep-ph/9808265]; F. de Campos *et al.*, Nucl. Phys. B **546**, 33 (1999) [arXiv:hep-ph/9710545].

[3] Q. R. Ahmad *et al.* [SNO Collaboration], Phys. Rev. Lett. **89**, 011302 (2002) [arXiv:nucl-ex/0204009]; S. Fukuda *et al.* [Super-Kamiokande Collaboration], Phys. Lett. B **539**, 179 (2002) [arXiv:hep-ex/0205075]. Phys. Rev. Lett. **81**, 1562 (1998) [arXiv:hep-ex/9807003]; see also talks by T. Kirsten, V. Gavrin, K. Lande and M. Smy at Neutrino 2002.

[4] C. S. Aulakh and R. N. Mohapatra, Phys. Lett. B **119**, 13 (1982); L. J. Hall and M. Suzuki, Nucl. Phys. B **231**, 41 (1984); G. G. Ross and J. W. Valle, Phys. Lett. B **151**, 375 (1985); J. R. Ellis *et al.*, Phys. Lett. B **150**, 142 (1985).

[5] M. Hirsch *et al.*, Phys. Rev. D **62**, 113008 (2000) [Erratum-ibid. D **65**, 119901 (2002)] [arXiv:hep-ph/0004115]; J. C. Romão *et al.*, Phys. Rev. D **61**, 071703 (2000) [arXiv:hep-ph/9907499]; M. A. Díaz *et al.*, arXiv:hep-ph/0302021, Phys. Rev. D, in press

[6] S. Y. Choi, E. J. Chun, S. K. Kang and J. S. Lee, Phys. Rev. D **60**, 075002 (1999) [arXiv:hep-ph/9903465]; D. E. Kaplan and A. E. Nelson, JHEP **0001**, 033 (2000) [arXiv:hep-ph/9901254]; C. H. Chang and T. F. Feng, Eur. Phys. J. C **12**, 137 (2000) [arXiv:hep-ph/9901260]; F. Takayama and M. Yamaguchi, Phys. Lett. B **476**, 116 (2000) [arXiv:hep-ph/9910320].

[7] M. A. Díaz, J. C. Romão and J. W. Valle, Nucl. Phys. B **524**, 23 (1998) [arXiv:hep-ph/9706315]; for a brief review see, e. g. J. W. Valle, in Proc. of International Symposium on Particles, Strings and Cosmology (PASCOS 98), pages 502-512, arXiv:hep-ph/9808292.

[8] A. Masiero and J. W. Valle, Phys. Lett. B **251**, 273 (1990); J. C. Romão, C. A. Santos and J. W. Valle, Phys. Lett. B **288**, 311 (1992); J. C. Romão and J. W. Valle, Nucl. Phys. B **381**, 87 (1992); K. Huitu, J. Maalampi and K. Puolamaki, Eur. Phys. J. C **6**, 159 (1999) [arXiv:hep-ph/9705406]; R. Kitano and K. Oda, Phys. Rev. D **61**, 113001 (2000) [arXiv:hep-ph/9911327].

[9] J. M. Mira, E. Nardi, D. A. Restrepo and J. W. Valle, Phys. Lett. B **492**, 81 (2000) [arXiv:hep-ph/0007266].

[10] A. Bartl *et al.*, Nucl. Phys. B **600**, 39 (2001) [arXiv:hep-ph/0007157], and references therein.

[11] W. Porod, M. Hirsch, J. Romão and J. W. Valle, Phys. Rev. D **63**, 115004 (2001) [arXiv:hep-ph/0011248], and references therein.

[12] M. Hirsch, W. Porod, J. C. Romão and J. W. Valle, Phys. Rev. D **66** (2002) 095006 [arXiv:hep-ph/0207334].

[13] H. Baer, M. Drees, F. Paige, P. Quintana and X. Tata, Phys. Rev. D **61**, 095007 (2000) [arXiv:hep-ph/9906233].

[14] A. Bartl *et al.*, Phys. Lett. B **384**, 151 (1996) [arXiv:hep-ph/9606256]; M. A. Díaz, D. A. Restrepo and J. W. Valle, Nucl. Phys. B **583**, 182 (2000) [arXiv:hep-ph/9908286]; D. Restrepo, W. Porod and J. W. Valle, Phys. Rev. D **64**, 055011 (2001) [arXiv:hep-ph/0104040].

[15] A. Bartl *et al.*, Nucl. Phys. B **502**, 19 (1997) [arXiv:hep-ph/9612436].

[16] A. G. Akeroyd *et al.*, Nucl. Phys. B **529**, 3 (1998) [arXiv:hep-ph/9707395]; F. de Campos *et al.*, Nucl. Phys. B **451**, 3 (1995) [arXiv:hep-ph/9502237].

[17] T. Banks, Y. Grossman, E. Nardi and Y. Nir, Phys. Rev. D **52**, 531 (1995); J. C. Romão *et al.*, Nucl. Phys. B **482**, 3 (1996) [arXiv:hep-ph/9604244]; M. Nowakowski and A. Pilaftsis, Nucl. Phys. B **461**, 19 (1996) [arXiv:hep-ph/9508271]; G. Bhattacharyya, D. Choudhury and K. Sridhar, Phys. Lett. B **355**, 193 (1995) [arXiv:hep-ph/9504314]; H. P. Nilles and N. Polonsky, Nucl. Phys. B **484**, 33 (1997) [arXiv:hep-ph/9606388]; A. Y. Smirnov and F. Vissani, Nucl. Phys. B **460**, 37 (1996) [arXiv:hep-ph/9506416]; B. de Carlos and P. L. White, Phys. Rev. D **55**, 4222 (1997) [arXiv:hep-ph/9609443].

[18] M. Maltoni, T. Schwetz, M. A. Tortola and J. W. Valle, Phys. Rev. D **67** 013011 (2003), [arXiv:hep-ph/0207227], and references therein. The e-Print Archive version of this paper has been updated to include the results of KamLAND.

[19] M. A. Díaz *et al.* Nucl. Phys. B **590**, 3 (2000) [arXiv:hep-ph/9906343], Phys. Lett. B **453**, 263 (1999) [arXiv:hep-ph/9801391]; A. G. Akeroyd, M. A. Díaz and J. W. Valle, Phys. Lett. B **441**, 224 (1998) [arXiv:hep-ph/9806382]; M. A. Díaz, E. Torrente-Lujan and J. W. Valle, Nucl. Phys. B **551**, 78 (1999) [arXiv:hep-ph/9808412]; M. A. Díaz, J. Ferrandis and J. W. Valle, Nucl. Phys. B **573**, 75 (2000) [arXiv:hep-ph/9909212].

[20] T. Gherghetta, G. F. Giudice and J. D. Wells, Nucl. Phys. B **559**, 27 (1999) [arXiv:hep-ph/9904378].

[21] J. W. Valle, "Standard and non-standard neutrino properties", Proc. of 20th International

Conference on Neutrino Physics and Astrophysics (Neutrino 2002), Munich, Germany, 25-30 May 2002, arXiv:hep-ph/0209047.

[22] M. C. González-García and Y. Nir, arXiv:hep-ph/0202058. For an updated review of neutrino properties after KamLAND, including also atmospheric data see S. Pakvasa and J. W. Valle, arXiv:hep-ph/0301061, invited contribution to the INSA special issue on Neutrinos.

[23] V. D. Barger, C. Kao and T.-J. Li, Phys. Lett. B**433**, 328 (1998) [arXiv:hep-ph/9804451]; V. D. Barger and C. Kao, Phys. Rev. D**60**, 115015 (1999) [arXiv:hep-ph/9811489].

[24] In the trilepton analysis, we reject events presenting more than three isolated charged leptons. In the R-parity conserving case, this procedure makes no difference.

[25] T. Söstrand, Computer Phys. Commun. **82**, 74 (1994).

[26] We have used the MADGRAPH PACKAGE, T. Stelzer and W. F. Long, Comput. Phys. Commun. **81**, 357 (1994).

[27] K. Hagiwara *et al.*, Phys. Rev. D66, 010001 (2002).

[28] This procedure differs from the one used in Ref. [13], which used only Gaussian statistics. The use of Poison statistics leads to more restrictive bounds.

[29] V. D. Barger, T. Han, S. Hesselbach and D. Marfatia, Phys. Lett. B **538**, 346 (2002) [arXiv:hep-ph/0108261].

[30] K. T. Matchev and D. M. Pierce, Phys. Rev. D **60**, 075004 (1999) [arXiv:hep-ph/9904282].

[31] In our model, any supersymmetric particle is a possible LSP candidate, since it is unstable and thus is not a cosmological relic. However, only the lightest neutralino leads to a signal cross section which can be large enough to be measurable at the Tevatron.

BG (fb)	σ (fb)
WZ (Z $\rightarrow \tau\tau$)	0.17
$W^*Z^*,W^*\gamma \rightarrow ll\bar{l}$	0.12
$W^*Z^*,W^*\gamma \rightarrow ll'\bar{l}'$	0.15
$t\bar{t}$	1.15
Z^*Z^*	0.05
total	1.64

TABLE I: Background cross sections in fb for the trilepton signal at the Tevatron Run II after kinematical cuts discussed in the text.

BG (fb)	σ (fb)
WZ	0.01
Z^*Z^*	0.10
$t\bar{t}$	0.16
total	0.27

TABLE II: Background cross sections in fb for the multilepton signal at the Fermilab Tevatron Run II after kinematical cuts discussed in the text.

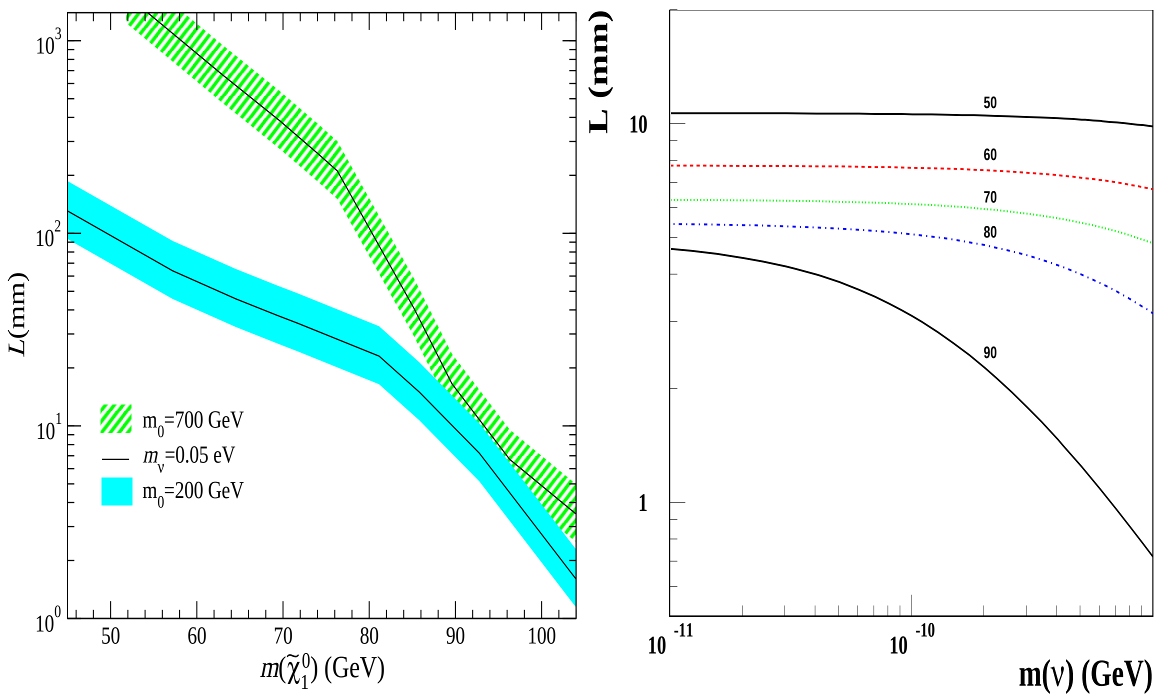

FIG. 1: $\tilde{\chi}^0_1$ decay length versus LSP mass for $A_0 = 0$, $\mu > 0$ and $\tan\beta = 3$ for (a) fixed BRpV parameters: $\epsilon_\tau = 0.22$ GeV, $m_{\nu_3} = 0.05$ eV (solid lines) and current atmospheric 3σ band (shaded bands); (b) as a function of the neutrino mass m_{ν_3} for $m_0 = 100$ GeV and several values of $\tilde{\chi}^0_1$ masses .

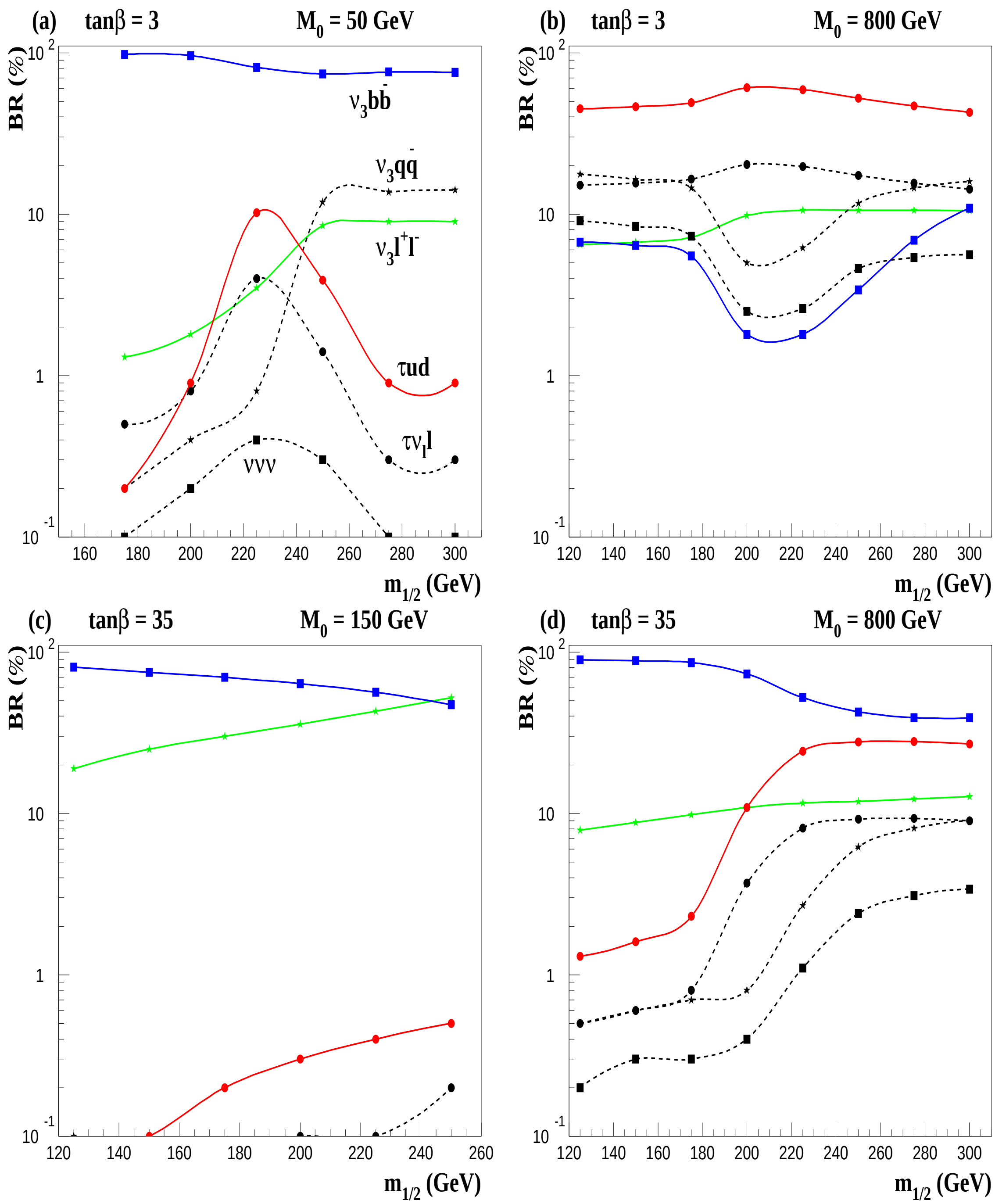

FIG. 2: $\tilde{\chi}^0_1$ branching ratios as a function of $m_{1/2}$ for $A_0 = 0$, $\mu > 0$, $\epsilon_\tau = 0.22$ GeV, and $m_{\nu_3} = 0.05$ eV. The solid lines denote $\tilde{\chi}^0_1 \to \nu_3 b\bar{b}$ (squares); $\tilde{\chi}^0_1 \to \tau u\bar{d}$ (circles); and $\tilde{\chi}^0_1 \to \nu_3 \ell^+\ell^-$ (stars). The dashed lines denote $\tilde{\chi}^0_1 \to$ invisible (squares); $\tilde{\chi}^0_1 \to \tau\nu_\ell\ell$ (circles); and $\tilde{\chi}^0_1 \to \nu_3 q\bar{q}$ (stars) .

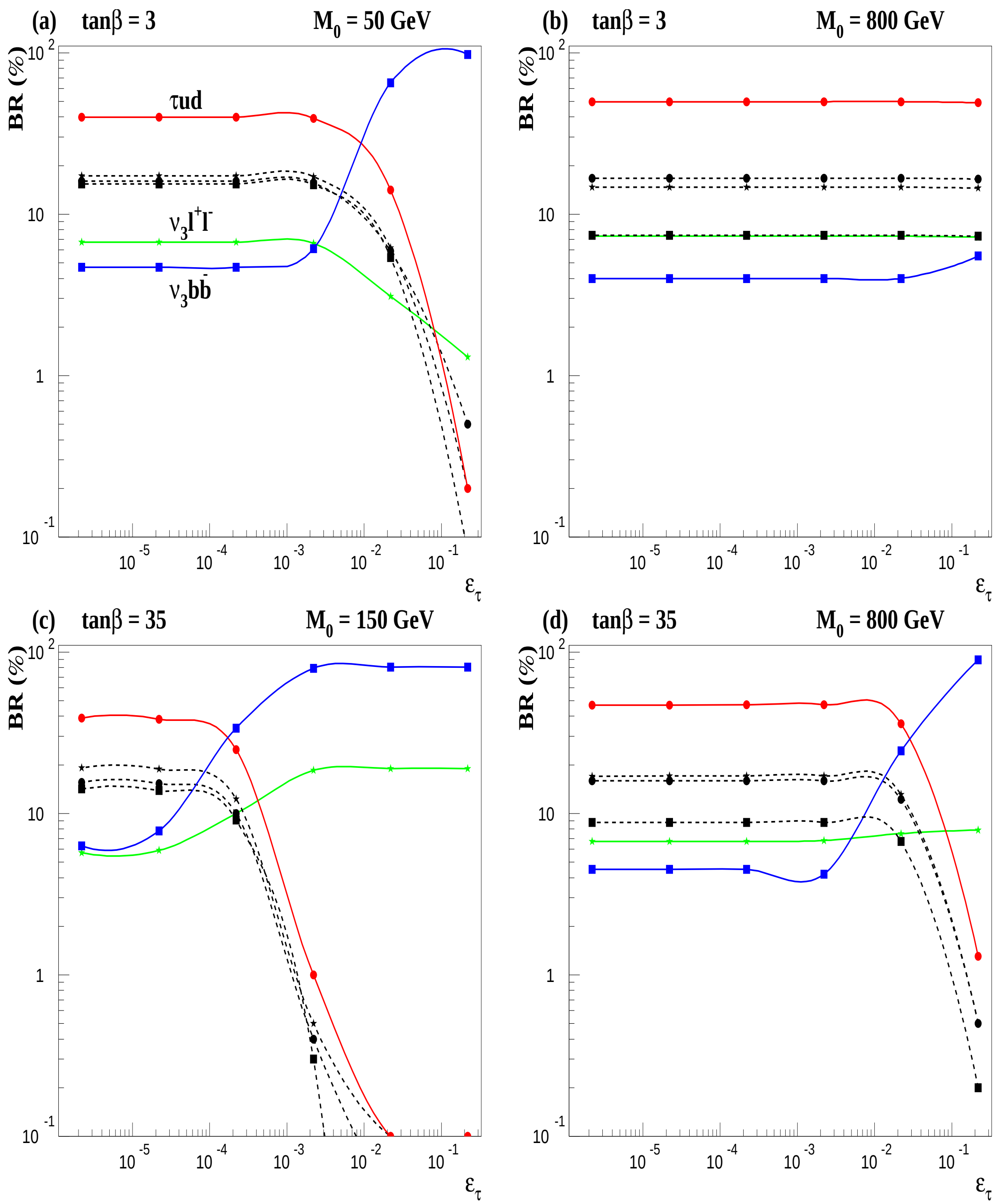

FIG. 3: $\tilde{\chi}^0_1$ branching ratios as a function of ϵ_τ for $A_0 = 0$, $\mu > 0$, and $m_{\nu_3} = 0.05$ eV. We fixed $m_{1/2} = 175$ GeV in the case of $\tan\beta = 3$ and $m_{1/2} = 125$ GeV for $\tan\beta = 35$. The lines are as in Fig. 2.

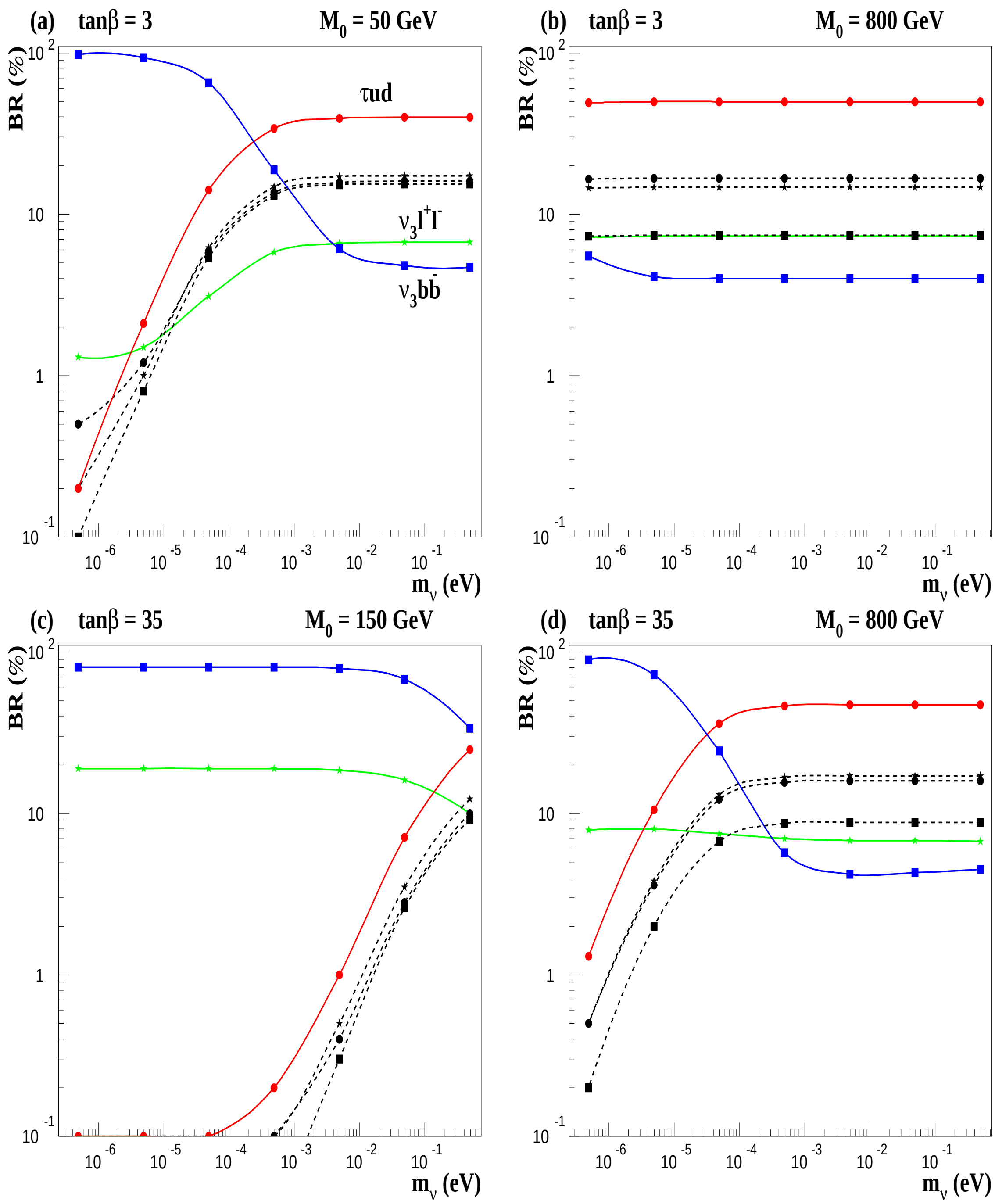

FIG. 4: $\tilde{\chi}^0_1$ branching ratios as a function of m_{ν_3} for $A_0 = 0$, $\mu > 0$, and $\epsilon_\tau = 7 \times 10^{-4}$ GeV. We fixed $m_{1/2} = 175$ GeV in the case of $\tan\beta = 3$ and $m_{1/2} = 125$ GeV when $\tan\beta = 35$. The lines are as in Fig. 2.

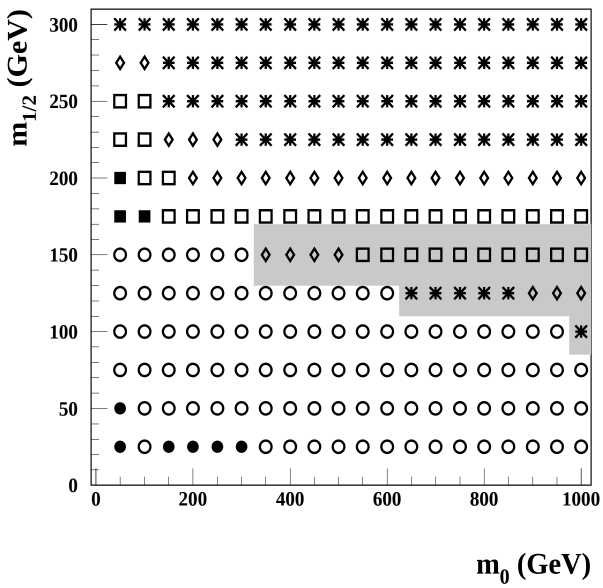

FIG. 5: Reach of Fermilab Tevatron Run II using the trilepton signal in the $m_0 \otimes m_{1/2}$ plane for $A_0 = 0$, $\tan\beta = 3$, $\mu > 0$, $\epsilon_\tau = 7 \times 10^{-4}$ GeV, and $m_{\nu_3} = 0.05$ eV. The black circles are theoretically excluded, while the white circles are experimentally excluded by sparticle and Higgs boson searches at LEP2. The black squares denote points accessible to Tevatron experiments at 5σ level with 2 fb^{-1} of integrated luminosity, while the white squares are accessible with 25 fb^{-1}. Points denoted by diamonds are accessible at the 3σ level with 25 fb^{-1}, while the stars correspond to the region not accessible to Tevatron. The long lifetime of the neutralino reduces considerably the signal in the shaded area, however, it suggests that the sensitivity can be improved by looking for displaced vertices.

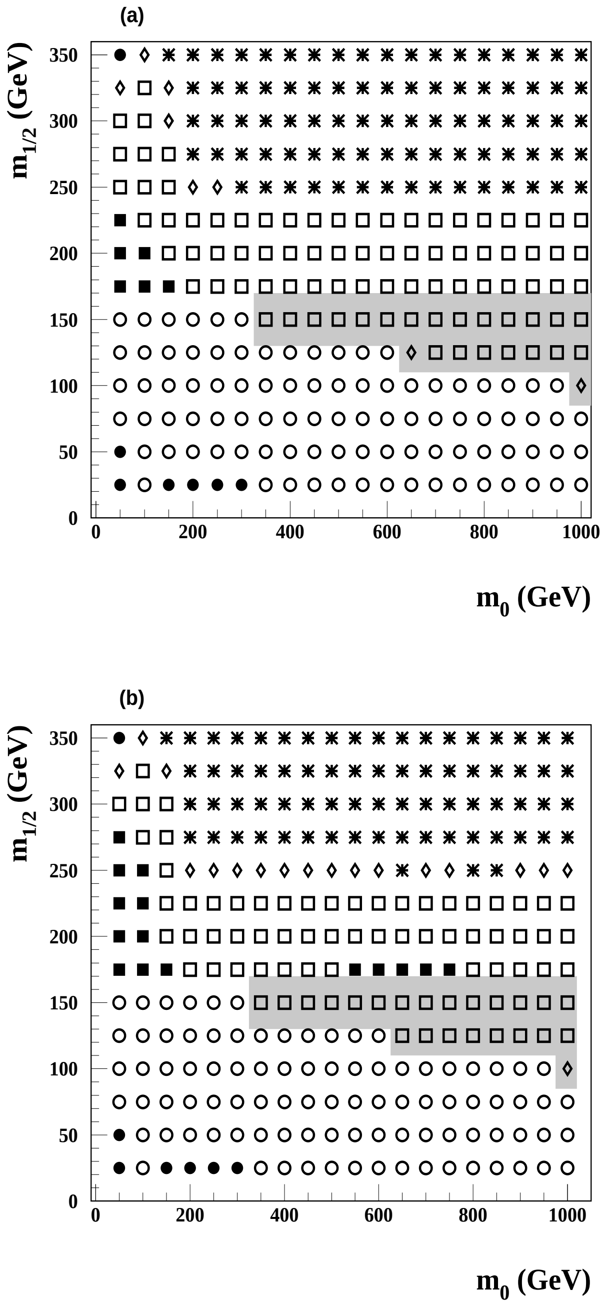

FIG. 6: (a) Reach of Fermilab Tevatron Run II in the 4 or more lepton channel. (b) Combined trilepton and multilepton results. All parameters and conventions were chosen as in Fig. 5.

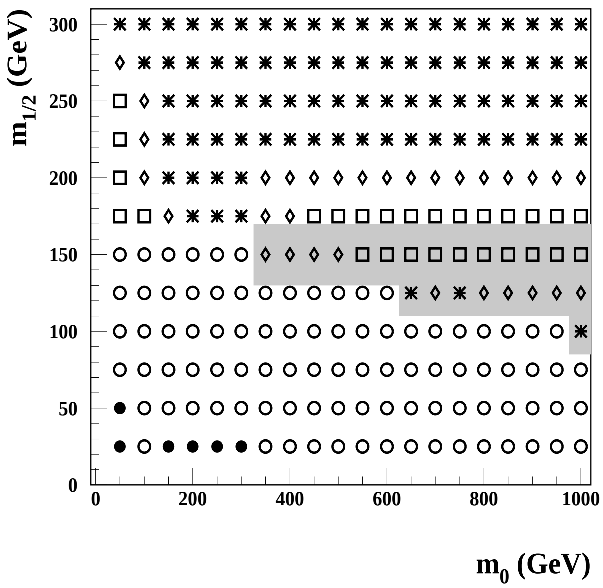

FIG. 7: Reach of Fermilab Tevatron Run II using the trilepton signal in the $m_0 \otimes m_{1/2}$ plane for $A_0 = 0$, $\tan\beta = 3$, $\mu > 0$, $\epsilon_\tau = 0.22$ GeV, and $m_{\nu_3} = 0.05$ eV. The conventions are the ones in Fig. 5.

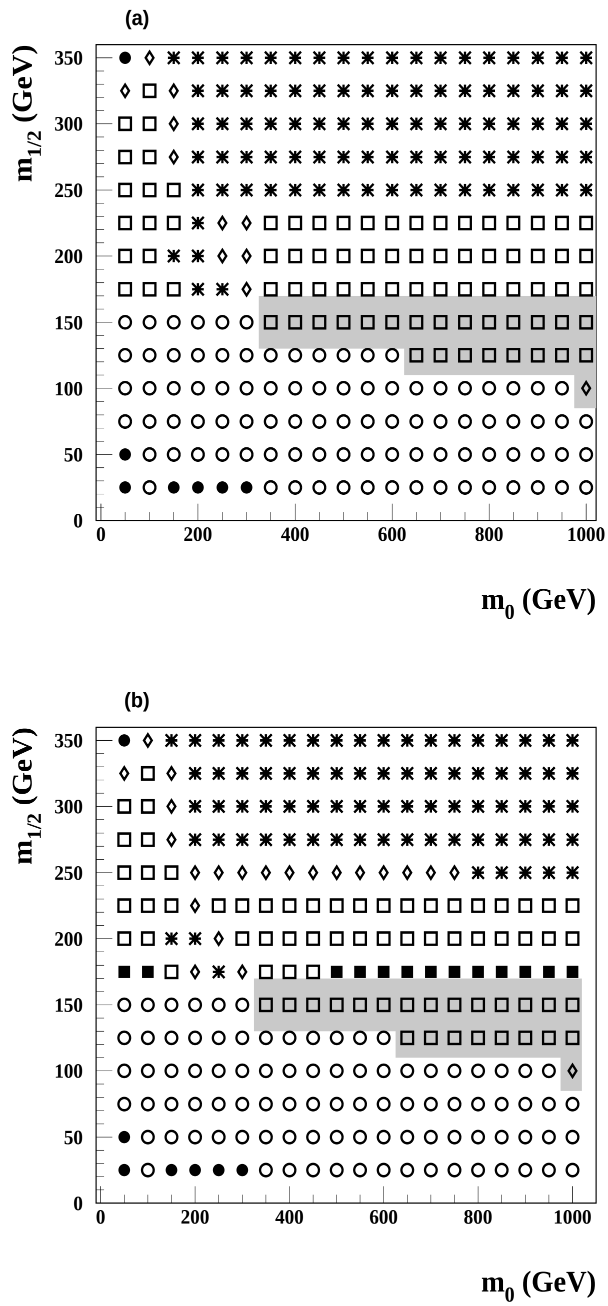

FIG. 8: (a) Reach of Fermilab Tevatron Run II in the 4 or more lepton channel. (b) Combined trilepton and multilepton results. All parameters were chosen as in Fig. 7.

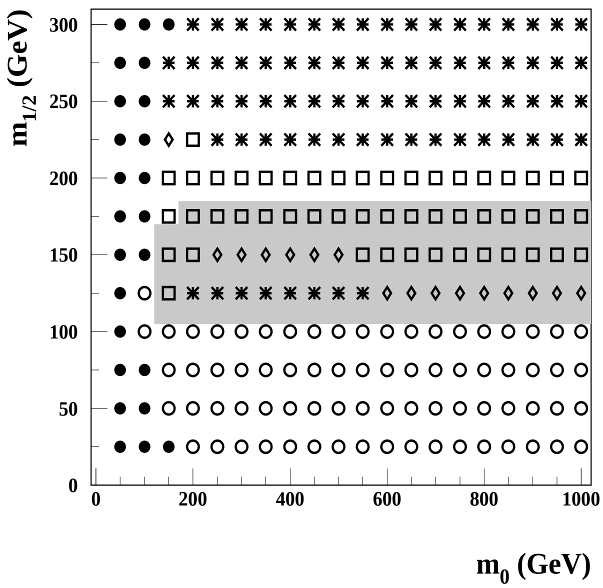

FIG. 9: Reach of Fermilab Tevatron Run II using the trilepton signal in the $m_0 \otimes m_{1/2}$ plane for $A_0 = 0$, $\tan\beta = 35$, $\mu > 0$, $\epsilon_\tau = 7 \times 10^{-4}$ GeV, and $m_{\nu_3} = 0.05$ eV. The conventions are as in Fig. 5.

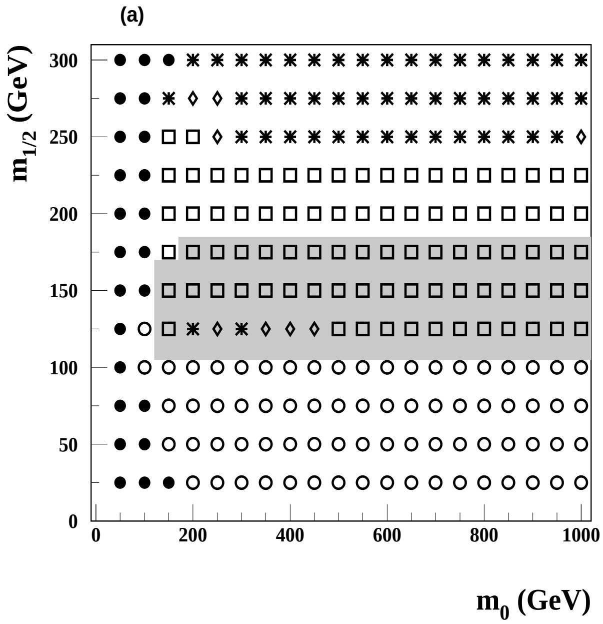

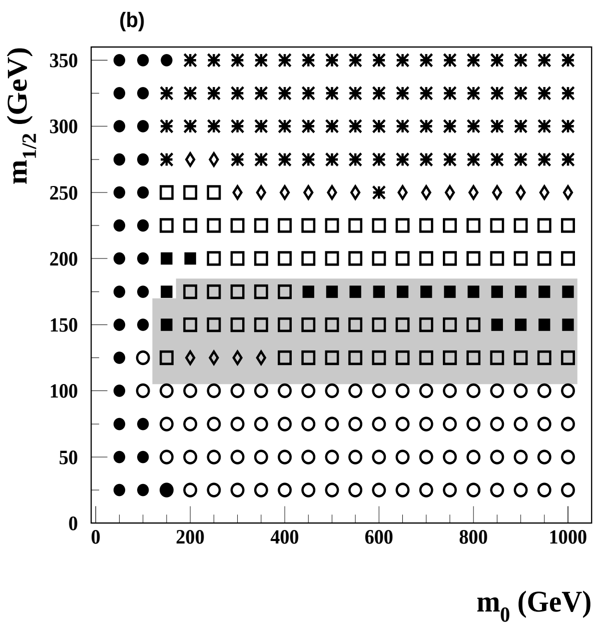

FIG. 10: (a) Reach of Fermilab Tevatron Run II in the 4 or more lepton channel. (b) Combined trilepton and multilepton results. All parameters were chosen as in Fig. 9.